Appl. Phys. B 80, 97–100 (2005)
DOI: 10.1007/s00340-004-1676-2

Applied Physics B
Lasers and Optics

V. GAYVORONSKY[1]
A. GALAS[1]
E. SHEPELYAVYY[1]
TH. DITTRICH[2]
V.YU. TIMOSHENKO[3,4]
S.A. NEPIJKO[1,✉]
M.S. BRODYN[1]
F. KOCH[4]

Giant nonlinear optical response of nanoporous anatase layers

[1] Institute of Physics NASU, pr. Nauki 46, 03028 Kiev, Ukraine
[2] Hahn-Meitner-Institute, Glienicker Str. 100, 14109 Berlin, Germany
[3] Moscow State University, Physics Department, Leninskie gory, 119992 Moscow, Russia
[4] Munich Technical University, Physics Department E16, James-Franck Str. 1, 85748 Garching, Germany

Received: 14 May 2004/Revised version: 1 September 2004
Published online: 17 November 2004 •

ABSTRACT A giant nonlinear optical response has been observed for nanoporous layers of titanium dioxide (anatase) under picosecond laser excitation with photon energy below the gap. At excitation intensity of 10 MW/cm^2 the nonlinear refractive index variation at the wavelength of 1064 nm corresponds to $\chi^{(3)} = 2 \times 10^{-5}$ esu which is six orders of magnitude higher than the respective value of bulk TiO_2. This effect is explained by resonant excitation of electronic states of defects at the developed surface of anatase nanoparticles.

PACS 42.65.-k; 73.20.At; 78.67.Bf; 81.07.Bc

1 Introduction

Nanocrystalline titanium dioxide is one of the most investigated materials for its unique physical and chemical properties. For example, nanocrystalline TiO_2 is applied in solar and fuel cells, protective and self-cleaning coatings, in catalysis and photocatalysis (see, for example, the review [1]). But also this material may become interesting for nonlinear optical (NLO) applications. In the transparency range of anatase (band gap $E_g = 3.2$ eV), the linear and NLO response of bulk anatase can be explained in terms of virtual transitions from the filled valence O $2p$ band to the empty cationic Ti $3d$ band [2]. Such a model predicts the typical for nonresonant processes nonlinear refractive index (NRI) variation due to the small magnitude of the cubic NLO susceptibility $\chi^{(3)} \sim 10^{-11}$ esu at the wavelength of 1 μm what is in good agreement with obtained experimental data [3, 4]. For low-dimensional systems, an enhancement of the NLO response was achieved in thin layers of oxides with transition-metal elements ($\chi^{(3)} \sim 10^{-8} \div 10^{-9}$ esu at 532 nm) while doping with electron donors or acceptors is important [5]. A large third-order NLO response $|\chi^{(3)}| \sim 10^{-6}$ esu was observed in Au:TiO_2 composite films for measurements on a fs time scale when the laser wavelength is close to the surface plasmon resonance [6]. Recently, a fast optical nonlinearity with a response time of 1.5 ps has been observed for anatase nanoparticles embedded in a polymer matrix [7] while these samples show a high positive refractive response $\mathrm{Re}(\chi^{(3)}) = 1.7 \times 10^{-9}$ esu and a high two-photon absorption (TPA) coefficient $\beta = 1.4$ cm/MW at 780 nm. For such samples, the value of β is larger by two orders of magnitude than for rutile single crystals measured at 532 nm [8, 9] due to a two-photon resonance with exciton transition. In this work, we show that values of even 2×10^{-5} esu can be reached for $\chi^{(3)}$ in nanoporous TiO_2. We named this effect a giant NLO response with respect to the values in bulk TiO_2.

✉ Fax: +38-044-2651589, E-mail: nepijko@yahoo.com

2 Experimental details

TiO_2 nanoparticles have been prepared by the sol-gel technique via controlled acid hydrolysis of titanium tetraisopropoxide (TIPT) in isopropanol [10]. Acetic acid was used as catalyst and polyethylene glycol PEG(1000) polymer was used as ligand for the TIPT and as complexing agent. Thin layers of TiO_2 nanoparticles were deposited on glass substrates by dip coating and consecutive annealing in air at 500 °C for 1 hour [11]. According to our ellipsometry data, the thickness of a thin layer of TiO_2 nanoparticles is $d = 180$ nm for one deposition cycle. The thickness of the layers of TiO_2 nanoparticles has been varied by repeating the deposition cycles. The layers of TiO_2 nanoparticles have excellent adhesion to the substrate and a high photocatalytic activity [11]. The high-resolution transmission electron microscopy has shown that nanoporous layers consist of a skeleton of nanoparticles. The maximum of the size (diameter) distribution is at 16 nm, the range of sizes comprises from 5 to 30 nm. The energy dispersive X-ray spectroscopy from separate nanoparticles has indicated that they contain titanium and oxygen. At last, analysis of the electron diffraction from these separate particles has revealed that they are pure anatase polymorp.

Figure 1 shows transmission spectra (recorded with a UV-VIS-NIR spectrometer Lambda 35 – Perkin Elmer) for thin layers of TiO_2 nanoparticles with $d = 180$ and 360 nm on the glass substrate (curves 1 and 2, respectively). Multiple interference in the thin layers of TiO_2 nanoparticles has been taken into account for the analysis of the transmission data. The scattering was negligible (less than 0.5% at 633 nm). The obtained optical band gaps are 3.42 and 3.63 eV for indirect and direct transitions, the fundamental absorption tail is 115 meV what is in good agreement with literature. Below the band gap, the absorption coefficient α is still relatively high for the given samples (400 and 950 cm^{-1} at 633 and 940 nm, respectively).

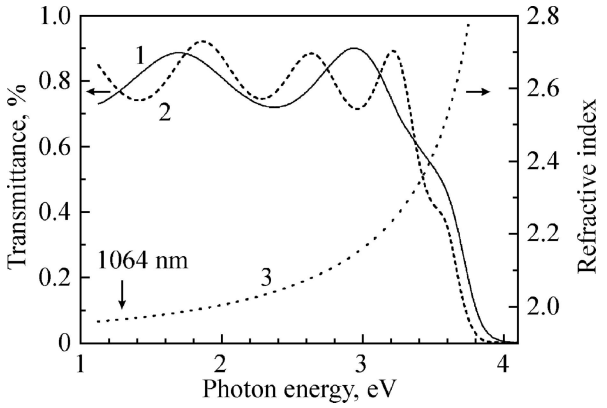

FIGURE 1 Transmission (*curves* 1 and 2) spectra and refractive index dispersion (*curve* 3) of thin layers of TiO_2 nanoparticles (layer thickness 180 nm – *curve* 1, 360 nm – *curve* 2)

The pronounced interference patterns allow us to determine the dispersion of the refractive index (Fig. 1, curve 3). The refractive index can be fitted by using the Sellmeir equation for a single oscillator [2]: $n^2 = n_0^2 + A/\left(E_s^2 - (h\nu)^2\right)$ with $n_0 = 1.773$, $A = 13$ and $E_s = 4.1$ eV. The porosity of the thin layers of TiO_2 nanoparticles ($32 \div 34\%$) was obtained by applying the two-component (anatase and voids) Bruggemann effective media approximation in the transparency region.

The laser beam self-action phenomena have been studied in thin layers of TiO_2 nanoparticles by using the far field spatial profile analysis technique [12]. In the experiment, the sample was positioned far beyond the focal plane 7 cm of the focusing lens $f = 11$ cm and was illuminated with a diverging Gaussian beam of a Nd:YAG laser (wavelength 1064 nm, duration time of a pulse 42 ps, repetition rate 3 Hz). For each laser shot, the light intensities were measured for the incident and transmitted laser pulses and for the pulse transmitted through an on-axis diaphragm in the far field (42.3 cm from the lens). The diameter of the beam spot was 0.7 mm at the sample in order to measure the NLO response in the range from 1 to 100 MW/cm^2 with a high signal to noise ratio. In addition, statistical averaging of about 10^4 laser shots has been performed for measuring the intensity dependence of the NLO response for one sample. The measurements were performed in ambient air at room temperature. The reversible character of the NLO response has been thoroughly controlled.

3 Experimental results and their discussion

Figure 2 presents the dependence of the total transmittance (a) and normalized on-axis transmittance (b) on the input laser intensity for layers of TiO_2 nanoparticles of thickness 180 and 360 nm (curves 1 and 2, respectively). At intensities below 10 MW/cm^2, photoinduced bleaching (darkening) has been observed for the layer with thickness of 180 (360) nm, see Fig. 2a. At intensities above 10 MW/cm^2, all investigated samples show photoinduced darkening, while the photoinduced absorption saturates at large intensities. The variation of the transmittance by few percent is accompanied with a pronounced changing of the beam radius and an essential enhancement of the on-axis transmittance in the far field

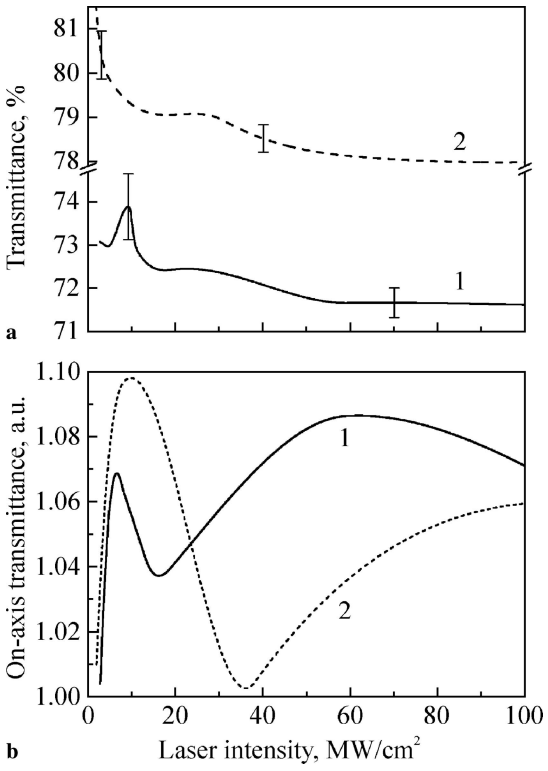

FIGURE 2 Dependence of the total transmittance (**a**) and of the normalized on-axis transmittance in far field (**b**) of thin layers of TiO_2 nanoparticles (layer thickness 180 nm – *curve* 1, 360 nm – *curve* 2) on the laser intensity at 1064 nm

(Fig. 2b), i.e., self-focusing of the laser beam in the layers is rather important.

The real (NRI variation) [13] and imaginary (photoinduced absorption) parts of the effective cubic nonlinearity $\chi^{(3)}$ can be obtained by assuming the simplest model for multiphoton processes. The normalized on-axis transmittance in the far field T_a through the aperture with radius r_0 can be expressed by taking into account a Gaussian decomposition approach [14] with subsequent spatial-temporal averaging [15]:

$$
\begin{aligned}
T_a(\varphi_{nl}) &= S\left\{1+\exp\left[\frac{-4r_0^2\left(3+b^2\right)}{w^2\left(9+b^2\right)}\right]\sin\left[\frac{8br_0^2}{w^2\left(9+b^2\right)}\right]\frac{\varphi_{nl}}{S\sqrt{2}}\right. \\
&\quad + \left(\exp\left[\frac{-6r_0^2\left(5+b^2\right)}{w^2\left(25+b^2\right)}\right]\cos\left[\frac{24br_0^2}{w^2\left(25+b^2\right)}\right]\right. \\
&\quad \left.\left. - \exp\left[\frac{-6r_0^2\left(1+b^2\right)}{w^2\left(9+b^2\right)}\right]\right)\frac{\varphi_{nl}^2}{3S\sqrt{3}}+\ldots\right\}, \qquad (1)
\end{aligned}
$$

where $S = 1 - \exp\left(-2r_0^2/w^2\right)$ is the aperture linear transmittance, $b = -(1 - z/R)/\left(ka^2/2z\right)$ is ratio of geometric focusing to diffraction broadening, $\varphi_{nl} = kd\Delta n$ is on-axis NLO phase shift due to the NRI variation Δn that is proportional to a peak laser intensity I_0, k is the wavevector, w is the beam radius in the linear regime, a is the beam radius at the sample plane, R is the wave front curvature at the sample plane and z is the distance between the sample plane and the aperture.

Equation (1) has been used to fit the normalized on-axis transmittance plotted in Fig. 2b. The estimated NLO cubic response is $\mathrm{Re}(\chi^{(3)}) \sim 2 \times 10^{-5}$ esu what is six (four) orders of magnitude higher than for the bulk (nanoparticle) response. This high NLO response can explain the different variation of the total transmittance for the layers with different thickness at intensities below 10 MW/cm^2.

The efficient modulation of the NLO phase changes the multiple beam interference conditions inside the nanoporous layer (NLO Fabry–Perot cavity effect). The positive NRI peak variation Δn (~ 1 at 7 MW/cm^2) leads to reduction of the wavelength in the thin layers of TiO_2 nanoparticles $\Delta\lambda = -\lambda\Delta n/n\,(\lambda)$ that causes linear transmittance increasing (decreasing) for the single (double) layer film in 1064 nm range, see Fig. 1. The effect corresponds to bleaching (darkening) versus laser intensity of the sample with the thickness 180 (360) nm at initial intensities, see Fig. 2a.

From a phenomenological point of view, the observed NLO can be described as an effective TPA process with an enhanced β coefficient. For instantaneous cubic NLO response, the total transmittance can be expressed as [15]

$$T\,(I_0) = T_{\mathrm{lin}}\frac{\ln\,(1+q)}{q}\left[\frac{1+0.228q}{1+0.136q}\right], \qquad (2)$$

where T_{lin} and $L_{\mathrm{eff}} = (1-\exp\,(-\alpha d))/\alpha$ are the linear transmittance and the effective interaction length. The value of the parameter q is given by $q = \beta L_{\mathrm{eff}} I_0$. The fraction in brackets in (2) is a proper approximation for the temporal averaging effect for a Gaussian temporal profile in the case of $q < 100$ range.

For the TiO_2 layer with thickness of 360 nm, rather high values of $\beta = 770$ cm/MW (at intensities below 3 MW/cm^2) and of $\beta = 100$ cm/MW (at intensities between 5 and 11 MW/cm^2) have been obtained. For comparison, β is $14 \div 18$ cm/GW for bulk TiO_2 (rutile) at 530 nm [8]. The value of β is about 300 cm/MW at the negative transmittance slope (intensity $11 \sim 13$ MW/cm^2) for the layer of TiO_2 nanoparticles with thickness 180 nm. From our point of view, the difference of the effective TPA coefficients for both layers at laser intensities around 10 MW/cm^2 is caused by the dominating contribution of the NLO cavity effect that has opposite signs for the different samples.

As mentioned above, the absorption coefficient is relatively high for the given samples. Therefore, the large value of $\chi^{(3)}$ can be explained by resonant excitation of deep defect states in the forbidden gap of anatase. The nature of these states is not matter of this article, they are related probably to surface states and/or oxygen vacancies. It should be remarked that the value of $\chi^{(3)}$ can be even further increased if additional defects are generated by slight reduction of the anatase at decreased partial pressures of oxygen. However, in such case, the action of intensive laser pulses would be accompanied by non-reversible changes in the layers of TiO_2 nanoparticles.

We believe that the resonant transition from the localized deep trap (DT) state into a shallow trap (ST) bound state with high electron polarisability is responsible for the giant NLO response in nanoporous TiO_2. Figure 3 depicts a schematic of the involved processes. The process "1" is given by the extremely fast excitation of an electron from DT into the conduction band CB followed by trapping into a ST (trapping within 180 fs [16]). Process "2" is an excitation and relaxation of electron from the CB to the ST. The relaxation of the excited electron back into a DT "3" is very slow (hundreds of ps [17]) in comparison to the used laser pulse. High rates of excitation and re-excitation and low rates of relaxation lead to a cumulative effect in terms of instantaneous response.

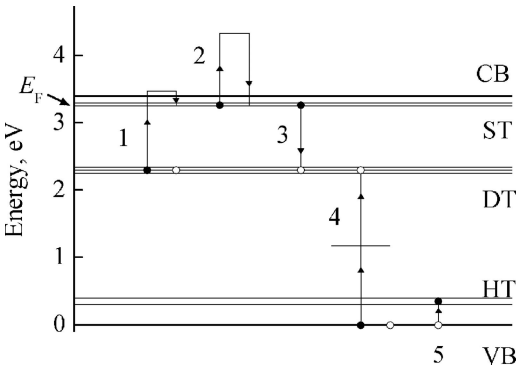

FIGURE 3 Scheme of involved basic processes (VB – valence band, CB – conduction band, E_F – Fermi-level, DT – deep traps, ST – shallow traps, HT – hole traps): 1 – resonant transition DT-CB with fast trapping at ST; 2 – excitation and relaxation of electron from CB to ST; 3 – resonant two-photon electron excitation from VB into DT through virtual state in the gap, creation of a free hole; 4 – electron trapping from ST into DT; 5 – free hole trapping, creation of surface bound holes

The resonant excitation of electrons from DT dominates at low laser intensities. At higher laser intensities, competitive resonant two-photon absorption of electrons from the valance band VB into empty DT "4" becomes important. This process starts to dominate around 20 MW/cm^2 when consequent photoinduced darkening takes place. As result, the values of β and $\mathrm{Re}(\chi^{(3)})$ decrease by 1–2 orders of magnitude. Photogenerated holes migrate to the surface where they are trapped at surface bound radicals "5" that create hole trap HT in the gap. At high laser intensities, Auger recombination will decrease further the NLO response.

The resonance conditions can be detuned by adsorption of the different types of molecules and by the variation of the active sites due to the adsorption/desorption processes. Analysis of the NLO response at higher excitation levels gives a possibility to get more detailed information about the photoinduced processes. From this point of view, the NLO response can be used to analyze surface states and their photocatalytic activity in systems of nanoparticles.

4 Conclusions

Finally, the giant NLO response of nanoporous anatase layers has been observed, and it has been attributed to the resonant optical depopulation of the deep defect states on the surface of TiO_2 (anatase) nanoparticles under picosecond laser irradiation. The result should have a simple physical background – some resonant cumulative effect in terms of instantaneous response, in our opinion. With respect to this, the effective readout of the cumulative NLO refractive index variation during the laser pulse at tens of ps has been observed.

ACKNOWLEDGEMENTS The work has been partially supported by the BMBF UKR 01/062 and SFFR F7/342-2001 of Ukraine grants.

The authors are grateful to A. Eremenko, N. Smirnova and I. Petrik for the prepared samples. V.Yu.T. acknowledges the support of the Alexander von Humboldt Foundation.

REFERENCES

1 U. Diebold: Surf. Sci. Rep. **48**, 53 (2003)
2 M.E. Lines: Phys. Rev. B **43**, 11 978 (1991)
3 R. Adair, L.L. Chase, S.A. Payne: Phys. Rev. B **39**, 3337 (1989)
4 T. Hashimoto, T. Yoko, S. Sakka: Bul. Chem. Soc. Jpn. **67**, 653 (1991)
5 M. Ando, K. Kadono, M. Haruto, T. Sakaguchi, M. Miya: Nature **374**, 625 (1995)
6 H.B. Liao, R.F. Xiao, H. Wang, K.S. Wong, G.K.L. Wong: Appl. Phys. Lett. **72**, 1817 (1998)
7 H.I. Elim, W. Ji, A.H. Yuwono, J.M. Xue, J. Wang: Appl. Phys. Lett. **82**, 2691 (2003)
8 A. Penzkofer, W. Falkenstein: Opt. Commun. **17**, 1 (1976)
9 Y. Watanabe, M. Ohnishi, T. Tsuchia: Appl. Phys. Lett. **66**, 3431 (1995)
10 N. Negeshi, K. Takeuchi: J. Sol-Gel Sci. Tech. **22**, 23 (2001)
11 V.Y. Gayvoronsky, A. Galas, D.Y. Manko, S.I. Lysenko, I. Petrik, N. Smirnova, A. Eremenko, Th. Dittrich, O. Loginenko, F. Koch: Proc. SPIE **5257**, 222 (2003)
12 M.S. Brodyn, A.A. Borshch, V.I. Volkov: *Refractive nonlinearity of wide-gap semiconductors and applications* (Harwood Acad. Publ., London 1990) p. 141
13 A.A. Borshch, M.S. Brodin, O.M. Burin, F.T. Vas'ko, V.Ya. Gaivoronskii: Bull. Acad. Sci. USSR Phys. Ser. **55**, 128 (1991)
14 D. Weaire, B.S. Wherrett, D.A.B. Miller, S.D. Smith: Opt. Lett. **4**, 331 (1974)
15 M. Sheik-Bahae, A.A. Said, T.-H. Wei, D.J. Hagan, E.W. van Stryland: IEEE J. Quantum Electron. **QE-26**, 760 (1990)
16 D.E. Skinner, D.P. Colombo Jr., J.J. Cavaleri, R.M. Bowman: J. Phys. Chem. **99**, 7853 (1995)
17 J.B. Asbury, R.J. Ellingson, H.N. Ghosh, S. Ferrere, A.J. Nozik, T. Lian: J. Phys. Chem. B **103**, 3110 (1999)